Agricultural and Forest Meteorology 297 (2021) 108270

Contents lists available at ScienceDirect

Agricultural and Forest Meteorology

journal homepage: www.elsevier.com/locate/agrformet

Performance of the ecosystem demography model (EDv2.2) in simulating gross primary production capacity and activity in a dryland study area

Hamid Dashti [a,*], Karun Pandit [b], Nancy F. Glenn [c,d], Douglas J. Shinneman [e], Gerald N. Flerchinger [f], Andrew T. Hudak [g], Marie Anne de Graaf [c], Alejandro Flores [c], Susan Ustin [h], Nayani Ilangakoon [i], Aaron W. Fellows [f]

[a] School of Natural Resources and the Environment, The University of Arizona, 1064 East Lowell Street, Tucson, AZ, 8572, USA
[b] School of Forest Recources and Conservation, University of Florida, 1745 McCarty Drive, Gainesville, FL 32611, USA.
[c] Department of Geosciences, Boise State University, 1910 University Dr, Boise, ID, 83725-1535, USA
[d] School of Civil and Environmental Engineering, University of New South Wales, Sydney, 2052, Australia
[e] USGS Forest and Rangeland Ecosystem Science Center, 970 Lusk St., Boise, ID, 83706, USA
[f] United States Department of Agriculture, Agricultural Research Service, 800 Park Blvd., Suite 105, Boise, ID, 83712, USA
[g] Rocky Mountain Research Station, U.S. Forest Service, 1221 South Main Street, Moscow, ID, 83843, USA
[h] Department of Land, Air, and Water Resources, University of California, Davis, CA, 93106-4060, USA
[i] Earth Lab, University of Colorado Boulder, Boulder, CO, 80303, USA

ARTICLE INFO

Keywords:
Drylands
GPP
Ecosystem demography model

ABSTRACT

Dryland ecosystems play an important role in the global carbon cycle, including regulating the inter-annual global carbon sink. Dynamic global vegetation models (DGVMs) are essential tools that can help us better understand carbon cycling in different ecosystems. Currently, there is limited knowledge of the performance of these models in drylands partly due to characterizing the heterogeneity of the vegetation and hydrometeorological conditions. The aim of this study is to evaluate the performance of a DGVM for drylands to facilitate improved understanding of gross primary production (GPP) as one of the important components of the carbon cycle. We performed a sensitivity analysis and calibrated the Ecosystem Demography (EDv2.2) DGVM to simulate GPP in a dryland watershed (Reynolds Creek Experimental Watershed, Idaho) in the western US for the years 2000-2017. GPP capacity and activity were investigated by comparing model simulations with GPP estimated from eddy covariance data (available from 2015-2017) and remote sensing products (2000-2017). Our results show good performance of EDv2.2 at daily timesteps ($RMSE \approx 0.38$ [kgC /m^2 /year]) between simulated and measured GPP in lower elevations of the watershed. Moreover, remote sensing analysis show that EDv2.2 captures the long-term trends in this ecosystem and performs relatively well in capturing phenometrics (start/end of the season). The performance of the model degrades in more productive sites with greater GPP (located at higher elevations in the watershed). To improve model performance, future studies will need to introduce additional plant functional types for drylands such as our study area, and modify plant processes (e.g., plant hydraulics and phenology) in the model.

1. Introduction

Dryland vegetation plays an important role in the global carbon budget, including regulating the global land carbon sink (Ahlström et al., 2015; Metcalfe, 2014; Poulter et al., 2014). Vegetation dynamics in drylands are largely a function of spatial and temporal variability in climate. For example, characteristic vegetation structure, composition, and function (e.g. photosynthesis) can differ markedly between lower and higher elevations in drylands, largely in response to corresponding differences in precipitation and temperature. Climate variability can also drive long-term changes in vegetation dynamics in dryland ecosystems. For example, climate change in the drylands of the Great Basin, US, may lead to a shift from winter snow to rain-dominated precipitation regimes, which in turn may favor fire-prone invasive species, such as cheatgrass (*Bromus tectorum*), that can convert native shrub-steppe communities to exotic annual grasslands (Concilio et al., 2013; Polley

* Corresponding author.
E-mail address: hamiddashti@email.arizona.edu (H. Dashti).

https://doi.org/10.1016/j.agrformet.2020.108270
Received 10 July 2020; Received in revised form 19 October 2020; Accepted 28 November 2020
Available online 15 December 2020

et al., 2013; Scott et al., 2015). These changes in structure and function ultimately affect ecosystem-scale vegetation productivity. Indeed, studies have shown that up to 60 percent of the global carbon sink anomaly can be explained by vegetation dynamics in dryland ecosystems (Ahlström et al., 2015; Poulter et al., 2014). This carbon sink variability is mostly associated with changes in gross primary production (GPP) (Yao et al., 2020). Thus, modelling the spatial and temporal dynamics of GPP in drylands is essential for global-scale studies on carbon balance and atmospheric CO_2.

GPP represents ecosystem-scale apparent photosynthesis and is a primary indicator of the vegetation state of an ecosystem. GPP can be assessed in terms of capacity (i.e., amount) and activity (i.e., dynamics) (Medvigy et al., 2013; Smith et al., 2018). Estimation of GPP at the ecosystem scale in drylands is helpful in understanding food and fiber availability, livestock grazing resources, and long-term processes related to the global carbon cycle (Ryu et al., 2019). However, there is a poor understanding of GPP in drylands due to variable hydrometeorological conditions (e.g., along an elevation gradient) and different plant functional types and photosynthetic pathways (e.g., C3 vs. C4) (Yan et al., 2019), among other factors. Direct measurement of GPP is a challenging task (Ryu et al., 2019; Yan et al., 2019) and commonly used products are based on data from eddy covariance (EC) towers, remote sensing, and dynamic global vegetation models (DGVMs) (for the latest review refer to Ryu et al., 2019). EC data provide the most reliable estimates of GPP capacity; however, in drylands the spatial distribution of EC towers is limited, and their time series may not be long enough to represent GPP dynamics. Remote sensing-based GPP derived from space-based sensors, such as MODIS (Running et al., 2004), provides long-term estimates that can be used for analysis of photosynthetic activity; however, GPP derived from remotely sensed data may be under- or overestimated depending on the ecosystem (Stocker et al., 2019; Verma et al., 2014), thus limiting our understanding of GPP capacity.

Process-based DGVMs are important tools to study GPP capacity and activity that can provide complementary observations to EC tower and remote sensing data. These models can provide simulations of photosynthesis at the leaf scale, as well as at the canopy and ecosystem scales. A wealth of studies have implemented DGVMs in different ecosystem types (see review in Fisher et al., 2018) to estimate GPP from local (EC towers) to regional scales. An evaluation of the DGVMs' performance prior to implementation should take place and include model parameterization, sensitivity analysis, calibration, and validation (Fer et al., 2018; Keenan et al., 2013; Kuppel et al., 2012; Pandit et al., 2019a; Post et al., 2017; Renwick et al., 2019; Santaren et al., 2007; Wang et al., 2001). However, there is an information gap in the evaluation of DGVMs in drylands and, more specifically, in dryland regions where vegetation productivity rapidly changes, especially across elevation gradients. Many studies have investigated the correlation between simulated GPP and GPP estimated from EC towers or remote sensing (Antonarakis et al., 2014; Pandit et al., 2019a; Renwick et al., 2019; Trugman et al., 2016). Comparing simulated GPP of drylands with EC towers is largely applicable to assessing GPP capacity rather than activity due to limited years of EC data. To fully capture GPP activity more specific metrics are required. Phenometrics, such as start of season (SOS) and end of season (EOS), and long-term trend analyses are examples of criteria that can be used for studying GPP activity (Chen et al., 2016; Forkel et al., 2015; Zhao et al., 2019).

The focus of this paper is on the Ecosystem Demography model version 2 (EDv2.2; Medvigy et al., 2009; Moorcroft et al., 2001). This model has been implemented in a variety of ecosystems (Antonarakis et al., 2014; Davidson et al., 2011; Kim et al., 2012; Levine et al., 2016; Lokupitiya et al., 2016; Medvigy et al., 2013, 2012; Trugman et al., 2016; Xu et al., 2016; Zhang et al., 2015) and, unlike most DGVMs, EDv2.2 represents the vertical and horizontal heterogeneity of terrestrial ecosystems (Longo et al., 2019b, 2019a). A further strength is that EDv2.2 accommodates the local variability of vegetation composition and structure. However, a thorough evaluation of this model in drylands is lacking. The heterogeneity and in many areas, the sparsity of vegetation in dryland communities, makes modeling these ecosystems challenging.

The objective of this study is to explore the ability of EDv2.2 to predict GPP capacity and activity in a dryland study area. To address this objective we (i) perform a sensitivity analysis and a state-of-the-art calibration method; (ii) assess GPP capacity by comparing the model output with EC tower data with varying vegetation productivity; and (iii) assess GPP activity by comparing long-term trends and phenometrics (SOS and EOS) between model GPP simulations and remote sensing data.

2. Materials and methods

2.1. Study area and data

The study area is Reynolds Creek Experimental Watershed (RCEW), located in the northern Great Basin of the western US (Fig. 1). In this study, we used three EC towers on the RCEW spanning an elevation range of ~1,000 m (Fig. 1, Table 1). With increasing elevation, mean annual precipitation increases and temperature decreases (Table 1; Flerchinger et al., 2019). The dominant vegetation cover of each EC site is a different species of sagebrush (*Artemisia* spp.) including Wyoming big sagebrush (*Artemisia tridentata* ssp. *wyomingensis*), low sagebrush (*Artemisia arbuscula*) and mountain big sagebrush (*Artemisia tridentata* ssp. *vaseyana*). The site dominated by Wyoming big sagebrush (WBS site) has the lowest elevation, the low sagebrush dominated site (LS site) occurs at mid-elevation, and the mountain big sagebrush site (MBS) has the highest elevation. Other vegetation at the WBS site includes green rabbitbrush (*Chrysothamnus viscidiflorus*), spineless horsebrush (*Tetradymia canescens*), perennial graminoids including bluebunch wheatgrass (*Pseudoroegneria spicata*), squirreltail (*Elymus elymoides*), and Sandberg bluegrass (*Poa secunda*), as well as nonnative cheatgrass (*Bromus tectorum*). The LS site includes predominantly Sandberg bluegrass, squirreltail, and Idaho fescue (*Fescue idahoensis*). Mountain snowberry (*Symphoricarpos oreophilus*) is another common shrub at the MBS site. Cheatgrass is less abundant at both LS and MBS compared to the WBS site, however at LS and MBS there is a strong presence of native forbs including longleaf phlox (*Phlox longifolia*), pale agoseris (*Agoseris glauca*), and silvery lupine (*Lupinus argentius*). A full description of each of these sites is presented in Flerchinger et al. (2019).

Vegetation field inventory data were collected during September–November of 2014 and May and June of 2015. The field data are publicly available (Glenn et al., 2017). Hourly meteorological forcing variables for the years 1988-2017 were obtained from the Weather Research and Forecast (WRF) model (Flores et al., 2016). The EC tower GPP data cover water years 2015-2017. We also used MODIS GPP products (MYD17A2H006) from 2000-2017.

2.2. EDv2.2 model calibration and sensitivity analysis

We implemented the EDv2.2 model at a point scale to correspond with the EC towers. In this model, at the static level the study area is divided into different sites based on the meteorological and abiotic (e.g. soil type) conditions. At the dynamic level, each site is divided into patches based on the time since last disturbance. Within each patch, individuals are grouped into cohorts based on plant functional type (PFT) and height of the plant (Fisher et al., 2018). The EDv2.2 model simulates vegetation dynamics based on the plant physiology associated with each PFT. Processes such as competition over resources (e.g. light and water) between PFTs, recruitment, and disturbance drive the ecosystem scale dynamics. The EDv2.2 model includes many sub-models to capture these processes. While a full description is outside the scope of this study, we describe in the SI the fundamental equations governing leaf physiology, which is directly related to GPP in the model. In addition, for the most recent review of different processes in EDv2.2, refer to

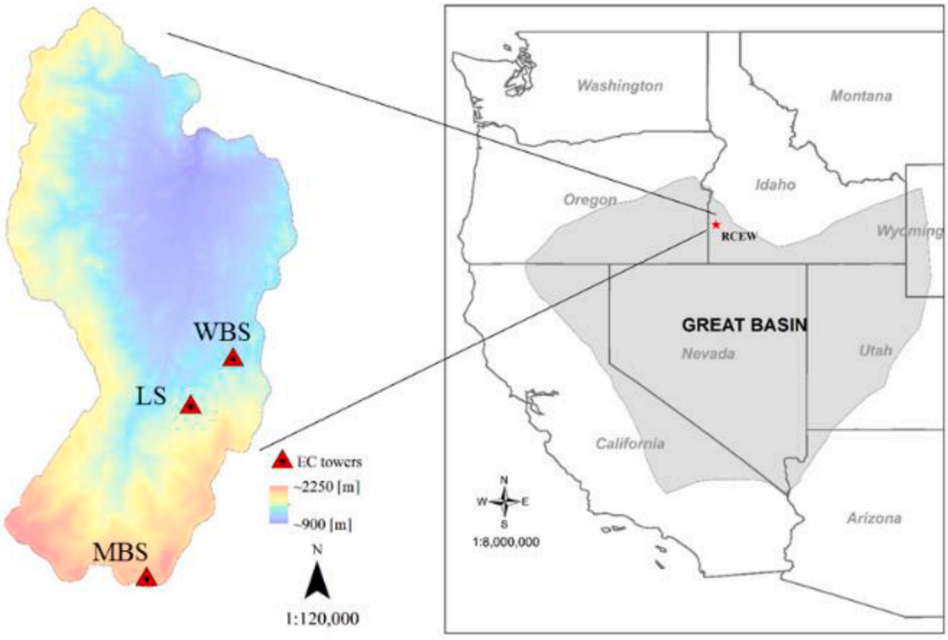

Fig. 1. Location of eddy covariance towers in Reynolds Creek Experimental Watershed, managed by US Department of Agriculture, Agricultural Research Service, Idaho.

Table 1
Site descriptions of the three eddy covariance tower sites, WBS, LS, MBS.

Site	Elevation [m]	Dominant vegetation cover	Mean annual precipitation [mm]	Mean annual temperature [°C]	Data availability [water year]
WBS	1188	Wyoming big sagebrush	307.94	9.75	2015-2017
LS	1618	Low sagebrush	367.42	9.02	2016-2017
MBS	2113	Mountain big sagebrush	586.15	4.58	2015-2017

Longo et al. (2019a). We utilize the shrub PFT parameters and allometric equations developed by Pandit et al. (2019) for the study area and meteorological forcing data based on the WRF model.

Due to differences in vegetation type and composition between the sites (Table 1), we implemented the calibration process at each site separately. We calibrated the model with regards to 12 parameters within EDv2.2 that are directly related to GPP (Table 2). One source of uncertainty in the calibration process is the increasing number of free parameters. To decrease this uncertainty, it is common to find non-influential parameters using a sensitivity analysis (SA) and exclude them from the calibration process. This is in accordance with Pareto's principle in which a model includes a few influential parameters, and a majority of non-influential parameters (Pappas et al., 2013). In this study, we used the Morris method for the sensitivity analysis. Multiple studies show that the results of a Morris SA are robust for calibration purposes (Hsieh et al., 2018; Janse et al., 2010; Tian et al., 2016). Morris returns the distribution of the elementary effect of each parameter on the model outputs. The absolute value of the mean (μ^*) of this distribution represents the influence of each parameter on the outputs (i.e. GPP in this study). The standard deviation (σ) is the variability of this influence, which is a function of model nonlinearity or parameter interactions (Campolongo and Saltelli, 1997; Saltelli et al., 2000; White

Table 2
GPP related PFT parameters within EDv2.2, their abbreviation, and initial, lower and upper boundaries selected for the Morris sensitivity analysis.

Parameter name [unit]	Abbreviation	Initial	Lower boundary	Upper boundary	Reference
Specific leaf area [m^2kg^{-1}]	SLA	4.5	2.0	15.0	(Brabec, 2014; Lambrecht et al., 2007; Olsoy et al., 2016; Pandit et al., 2019a)
Maximum carboxylation rate [$\mu molm^{-2}s^{-1}$]	VM0	16.5	4.0	30.0	(Comstock and Ehleringer, 1992; Oleson et al., 2013; Pandit et al., 2019a)
Stomatal slope	STO_S	7.0	2.0	15.0	(Bonan et al., 2014; Dietze et al., 2014; Pandit et al., 2019a)
Ratio of fine root to leaf biomass	Q_RATIO	3.2	0.4	12.0	(Dietze et al., 2014; Pandit et al., 2019a)
Root turnover rate [a^{-1}]	FTR	0.33	0.1	2.0	(GILL and JACKSON, 2000; Pandit et al., 2019a)
Leaf turnover rate [a^{-1}]	LTR	1.0	0.1	2.0	(Pandit et al., 2019a)
Growth respiration factor	GRESP	0.33	0.11	0.66	(Pandit et al., 2019a; Wang et al., 2013)
Cuticular conductance [$\mu molm^{-2}s^{-1}$]	CUT_C	1000.0	100.0	10000.0	(Barnard and Bauerle, 2013; Duursma et al., 2019; Pandit et al., 2019a)
Water conductance [$ms^{-1}kgCroot^{-1}$]	WAT_C	1.900000E-05	1.90E-06	1.90E-4	(Pandit et al., 2019a)
Seedling mortality	S-MOR	0.95	0.25	0.99	(Trugman et al., 2016)

et al., 2019). We follow the common approach of presenting the individual importance of a set of variables and associated interactions by plotting the μ* vs. σ from the Morris SA. In the next step, we calibrate the model using the PEST++ package (White et al., 2019) and the most influential parameters resulting from the SA. The calibration method is based on Tikhonov regularization and truncated singular value decomposition (SVD) regularization (Doherty, 2005; Fang et al., 2019) (refer to SI for more details). The SVD regularization enables us to incorporate the user's knowledge of the parameters. We used the values of the parameters provided in Table 2 as our initial approximations and lower/upper boundaries to constrain the PEST++ calibration.

2.3. EDv2.2 model evaluation

After calibrating the model, the performance of EDv2.2 in simulating GPP capacity and activity was tested using the EC tower data and MODIS GPP, respectively. In order to evaluate the model in terms of its performance to estimate GPP capacity, we calculate the Root Mean Square Error (RMSE) between GPP simulated from EDv2.2 and GPP observed from the EC towers. Since the EC tower data are temporally limited (Table 1), a meaningful time series analysis is challenging. Thus, for model evaluation of GPP activity, we compare the phenometrics (SOS and EOS), and long-term trend retrieved from the calibrated model simulations, and MODIS GPP for the 2000-2017 time period. Estimation of SOS and EOS is based on a weighted cross-correlogram spectral matching-phenology (CCSM-P; Chen et al., 2016). To compare the simulated start of season (SOS_S) and MODIS start of season (SOS_M), we calculate the mean absolute deviation ($MAD = (\sum|SOS_S - SOS_M|)/n$) where n is the number of observations year (i.e. 17 years). The same method was used for comparing EOS. The trend analysis is based on the recently developed Bayesian Estimator of Abrupt change, Seasonal change, and Trend algorithm (BEAST; Zhao et al., 2019). BEAST returns the non-linear trend in a time series and is able to decompose it into its seasonal and trend components; due to its Bayesian nature it returns confidence intervals on these components. We compared the long-term trends in model-simulated and MODIS GPP. For both phenology and trend analyses, we aggregated the daily model-simulated and MODIS GPP into monthly values based on the maximum composition approach (Forkel et al., 2015; Holben, 1986). More details on the CCSM-P and BEAST can be found in the SI.

3. Results

The results of the Morris sensitivity analysis (SA) are shown in Fig. 2. Among all parameters, the specific leaf area (SLA), stomatal slope (STO_S), cuticular conductance (CUT_C), and maximum carboxylation rate (VM0) show the highest individual influence (μ*). These parameters also show the largest non-linear influence and interaction effect at all sites (σ). The results from the other eight parameters indicate that EDv2.2 is less sensitive to them in simulating GPP (e.g. clustering near the lower left corner of Fig. 2). All four parameters indicated as influential are indeed used in the photosynthesis sub-model of EDv2.2, which is directly related to GPP (see SI). The stomatal slope is a fixed parameter in the stomatal conductance model (Leuning, 1995), which actively regulates the photosynthesis rate (Dietze et al., 2014). Cuticular conductance in EDv2.2 is equal to stomatal conductance when plants shut down their stomata due to environmental stress (Medvigy et al., 2009b; Moorcroft et al., 2001). The maximum carboxylation rate is maximum photosynthesis at 15°C based on the photosynthesis model developed for C3 plants (Farquhar et al., 1980). Finally, the specific leaf area scales leaf-level photosynthesis to the canopy-level (Dietze et al., 2014). Following our framework, we used these four parameters (SLA, STO_S, CUT_C, and VM0) for calibration analysis with PEST++.

Table 3 shows the corresponding standard deviation (STDV) and confidence intervals (upper/lower bounds) of the estimated parameters. Table 4 shows the calibration/validation RMSE between simulated and estimated GPP from EDv2.2 and the EC towers, respectively. We exclude MBS (highest elevation site) from Table 4 because the EDv2.2 calibration process resulted in no vegetation growth (zero GPP) for this site. This is because the estimated parameter values for this site are incorrect (Table 3). For example, the confidence interval for the SLA of this site is much large than the other sites and includes unrealistic negative numbers, providing evidence that the MBS site parameters are not reliable. We also found a higher STDV and wider confidence interval at the LS site for all of the parameters in comparison to the WBS site (lowest elevation). With this information, we conclude that the best EDv2.2 performance of GPP capacity is attained for the WBS site. Subsequently, all further analyses are performed for the WBS site only.

Fig. 3 shows simulated vs. observed (EC tower) GPP at WBS site. The mean annual observed and estimated GPP at this site is 0.38 [kgC/m^2/year] and 0.30 [kgC/m^2/year], respectively. Note that the model underestimated GPP for the 2017 water year, when observed GPP is higher than average.

In addition, we analyzed the contribution of the two dominant PFTs (shrub and grass) to total simulated GPP at the WBS site (Fig. 4). This allowed us to understand EDv2.2's capability to capture local vegetation heterogeneity.

We base our time series analysis for evaluating long-term performance of EDv2.2 on GPP activity at the WBS site. In order to evaluate GPP activity, we estimated SOS and EOS for the MODIS GPP and simulated GPP (Fig. 5). Visually, there is a good agreement between MODIS and EDv2.2, but with more agreement between simulated and

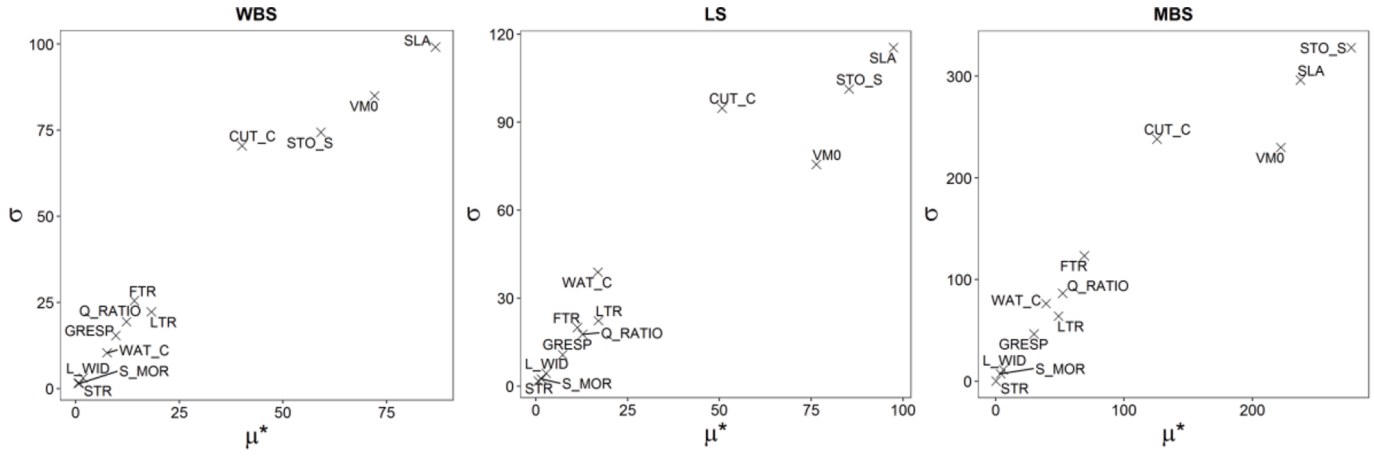

Fig. 2. Morris sensitivity analysis for WBS, LS, and MBS, μ* and σ are the mean and standard deviation of elementary effects. Based on this analysis, SLA, STO_S, CUT_C, and VM0 are identified as the most important parameters to estimate GPP at all three sites.

Table 3
Calibration results using PEST++ for SLA, STO_S, CUT_C, and VM0 and their uncertainty. STDV is standard deviation of the estimated parameters.

Parameter	WBS Best	STDV (upper bound; lower bound)	LS Best	STDV (upper bound; lower bound)	MBS Best	STDV (upper bound; lower bound)
SLA [m^2kg^{-1}]	6.14	0.03 (6.04;6.18)	7.50	0.47 (6.55;8.45)	2.82	3.25 (-3.67;9.32)
VM0 [$\mu molm^{-2}s^{-1}$]	24.50	0.21 (24.06;24.93)	19.45	0.48 (18.48;20.43)	7.44	2.04 (3.33;11.51)
STO_S	13.97	0.03 (13.90;14.05)	9.85	0.53 (8.77;10.92)	7.82	1.98 (3.83;11.76)
CUT-C [$\mu molm^{-2}s^{-1}$]	999.51	112.184 (775.143;1223.88)	1000	462.68 (74.62;1925.37)	1000	267.44 (465.121;1534.89)
Number of model runs	166	—	56	—-	failed	

Table 4
Calibration and validation results for EDv2.2 at the WBS and LS sites.

Site	RMSE (daily; monthly) [kgC/m^2/year] Calibration	Validation
WBS	0.22; 0.18	0.44; 0.38
LS	0.29; 0.24	0.47; 0.39

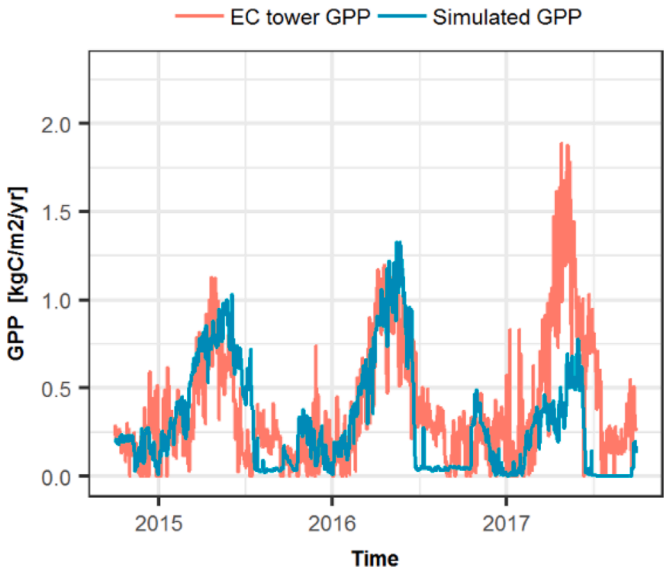

Fig. 3. Model simulations and EC tower-based observations of GPP for years 2015 through 2017 at the WBS site.

MODIS SOS (MAD = 18.6) compared to EOS (MAD = 25.2).

The results of the trend analysis using the BEAST algorithm are shown in Fig. 6. There is general agreement between MODIS and EDv2.2 during greening events, specifically in years 2011 and 2017. We also calculated the trend components of precipitation for the WBS site (2000-2017). The precipitation trend increases in years 2005, 2011 and 2017, leading to an increase in both simulated and MODIS GPP. However, there is a significant difference in the intensity of senescing events. For example, between 2000 and 2004, MODIS shows no trend in GPP whereas the EDv2.2 shows a significant trend. In general, the senescing and greening events are more intensified in the EDv2.2 simulations than in the MODIS GPP.

4. Discussion

4.1. Model calibration and sensitivity analysis

We compared parameters identified here with other studies in RCEW (Pandit et al., 2019a; Renwick et al., 2019). Three of the four influential parameters in this study (SLA, STO_S and VM0) are similar to those identified by Pandit et al., 2019. However, only SLA was identified as important by Renwick et al. (2019). These parameter discrepancies among studies may be due to the SA method or the DGVM structure. For example, in Pandit et al. (2019), a local SA was used in comparison to the Morris SA used here. In Renwick et al. (2019), the shrub PFT parameters for the LPJ-GUESS model were analyzed using a ranked partial correlation coefficient. In addition to these methods, the structure of the LPJ-GUESS model is different from EDv2.2. Thus, differences in SA between studies are expected, and one should consider the SA method and model structure when evaluating any DGVM model performance. Considering the wide range of DGMVs, intercomparison SA studies can highlight model limitations (e.g. structural issues) and help direct further improvements (Cariboni et al., 2007; Jakeman et al., 2006; Pappas et al., 2013). While a comprehensive intercomparison SA was

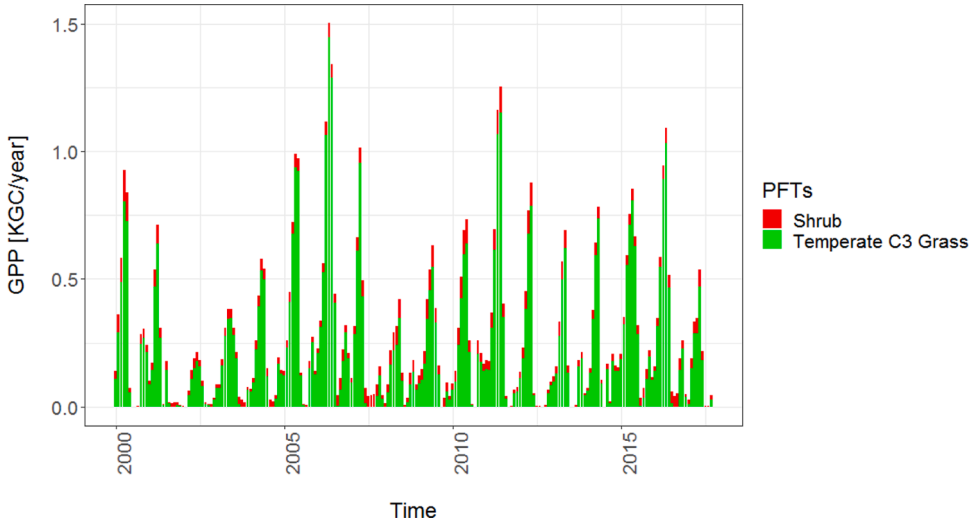

Fig. 4. Contribution of shrub and grass PFTs to total GPP at the WBS site.

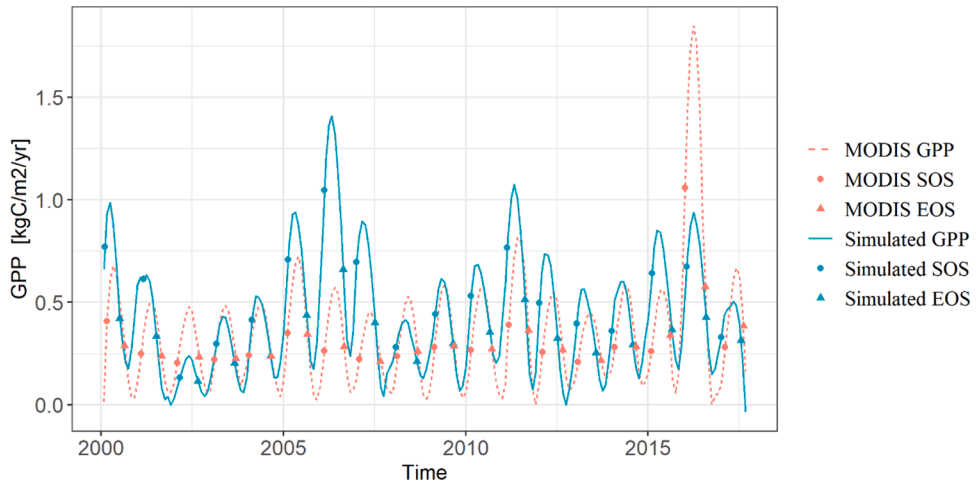

Fig. 5. Phenometrics estimated from MODIS GPP and simulated GPP using EDv2.2 at the WBS site.

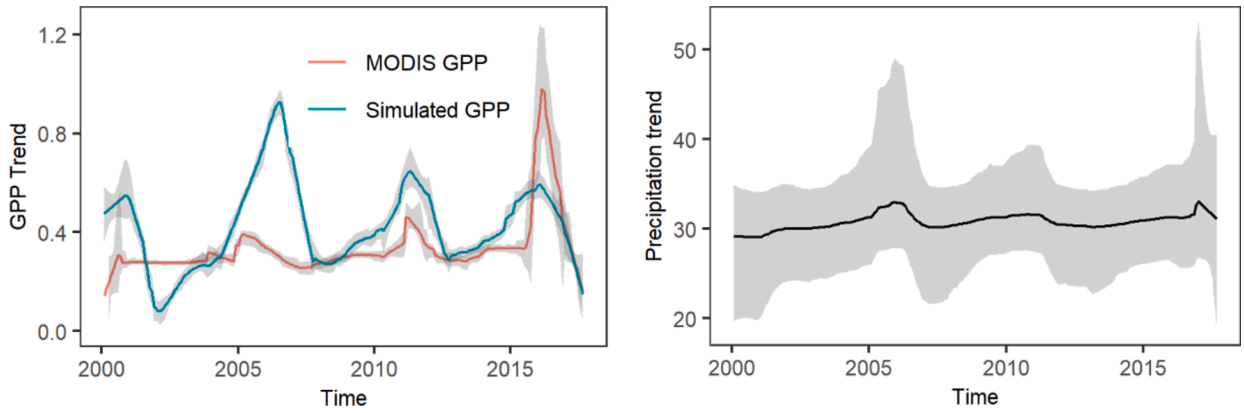

Fig. 6. Estimated trend component and its 95% confidence interval (gray shading) for MODIS and EDv2.2 GPP (left) and precipitation (right) for years 2000-2017 at the WBS site.

beyond the scope of this study, our results may be used alongside others for future model improvements.

From a methodological point of view, PEST++ is a gradient-based method which mathematically searches for local minima in the objective function space (Doherty, 2005; White et al., 2019). Being trapped in local minima is one of the drawbacks of gradient-based methods in cases where the model is highly nonlinear. In general, global calibration methods such as Covariance Matrix Adaptation Evolution Strategy (Hansen et al., 2003), Differential Evolution (Storn and Price, 1997), Particle Swarm Optimization (Li et al., 2020), and Bayesian approaches (e.g. Dietze et al., 2014; Fer et al., 2018) are preferable if their computational cost can be afforded. It should be noted that the short time span of the calibration process may impact the results. For example, the influence of other parameters such as root:shoot ratio and turnover rates may have a stronger influence on the GPP simulations over longer terms (decades). Precipitation during years used for calibration (2015-2016) was close to the long-term average, while precipitation for 2017 was above average. Underestimation of GPP during 2017 may imply that the calibration time period is insufficient to properly parameterize these variables for application beyond the range of conditions encountered during 2015-2016. Thus, increasing the calibration time period and introducing more anomalies (e.g. precipitation below or above the long-term average) should improve model performance. Further investigations should explore the influence of other factors over the longer term.

4.2. EDv2.2 GPP capacity and activity

EDv2.2 performed well in capturing GPP capacity (Table 4) at the WBS site with low vegetation productivity; however, the model performed more poorly at LS and MBS where vegetation productivity is higher. Also, GPP was underestimated for the WBS site in 2017 when the EC data indicated that GPP was higher than during previous years (Fig. 3). The less robust EDv2.2 model simulations of GPP at more productive, higher elevation sites may be discussed in terms of uncertainty in the model parameters (e.g. Table 3) and processes such as photosynthesis in the model structure. Shiklomanov et al., 2020 found that in forest ecosystems in the Upper Midwest of the US, the model parameters had a higher contribution to the overall uncertainty of EDv2.2 outputs than the model structure. DGVMs are heavily studied in forest ecosystems and the representation of different processes in models is well-developed. Thus, the higher contribution of model parameters to uncertainty may be expected for forest ecosystems. However, the poor performance and failure of EDv2.2 at more productive sites in our study is likely related to model processes. We suggest this because our study used PEST++ as a robust calibration method for the model parameters (Doherty, 2005; Fang et al., 2019). Further, considering that DGVMs are less studied in drylands, model representation of processes is not as mature as in other ecosystems. Consequently, the higher contribution of model structure to the uncertainty is not surprising. Our finding is in agreement with a recent study which showed that in a dryland study area, model structure contributed more than the parameters to the improvement of DGVMs (Li et al., 2020). One of the key factors which is

directly related to the EDv2.2 model structure is the lack of ecosystem heterogeneity represented in the model. At the WBS site, the main vegetation cover types are shrub and grass, and EDv2.2 reasonably captured the contribution of these PFTs to GPP over time (Fig. 4). As elevation increases at RCEW, the heterogeneity of the ecosystem also increases (Flerchinger et al., 2019). For example, the presence of forbs at MBS is noteworthy and significantly contributes to the carbon budget including GPP (Flerchinger et al., 2010). Currently, there is no PFT for forbs in EDv2.2. The lack of forbs and other PFTs common in higher-elevation drylands (e.g. juniper and aspen trees) in EDv2.2 may partly explain the poor performance of the model in capturing photosynthesis capacity at higher elevation and more productive sites. Thus, developing other PFTs commonly found at higher productive sites will likely improve model performance at those sites.

Other model processes are likely to influence the performance of DGVMs in drylands. For example, the water flux from the soil to plants and its distribution within the plant (i.e. plant hydraulics) play an important role in the performance of DGVMs in drylands (De Kauwe et al., 2015; Li et al., 2013, 2012; MacBean et al., 2019; Swenson and Lawrence, 2014). Flerchinger et al. (2019) found that the timing of complete snowmelt and water availability is a strong control on GPP at the MBS site. To what extent the EDv2.2 model captures this timing of water availability remains an open question. The interaction between shrubs and soil moisture availability in topographically complex shrubland environments (e.g. LS and MBS sites) is complicated. For example, previous studies have shown that the roots of dead plants contribute to water infiltration, improving dry soil moisture conditions and thus plants productivity (Wu et al., 2020, 2019). While plant mortality in EDv2.2 is accounted for, to our knowledge, there is limited understanding of this mechanism in drylands, hence the need for improvement in the model. We should also note that regulating photosynthesis (hence GPP) as a function of soil moisture in EDv2.2 is controlled by an empirical soil-moisture-dependent scaling factor (Longo et al., 2019b). Some studies have shown that modifying plant hydraulics greatly enhances the performance of DGVMs in drylands (Li et al., 2013, 2012; MacBean et al., 2019) and dry forests (Xu et al., 2016). In sum, the potential for model improvement by using more realistic, mechanistic plant hydraulics that consider water fluxes between plants and soil, and within plants in shrublands, needs further investigation.

Capturing phenology is also a challenging task for most DGVMs (Migliavacca et al., 2012; Richardson et al., 2013). The ED2.2 model performed relatively well compared to similar studies (e.g., Forkel et al., 2015). The difference between estimated phenometrics from MODIS and EDv2.2 may be due to a combination of uncertainty in remote sensing data, EDv2.2 model structure, and the method used for the retrieval of SOS and EOS. In general, GPP estimated from EC towers is considered more reliable than model-driven, remotely sensed GPP. However, long-term EC tower GPP data are lacking at RCEW. Which remote sensing dataset to use for phenological studies remains an open question. It has been shown that solar induced fluorescence (SIF) may better capture the dynamics of drylands (Smith et al., 2018), and future studies could explore the potential of comparing SIF with EDv2.2 results (SIF data were not available for the 2000-2017 time frame assessed here). The cold deciduous phenology subroutine in EDv2.2 used in this study is based on changes in seasonal temperature (Botta et al., 2000), when deciduous plants drop their leaves. In reality, the phenology of sagebrush (dominant shrub in WBS site) is more complicated. Sagebrush is semi-deciduous and keeps some leaves during the cold season (Evans and Black, 1993; Williams et al., 1997). Renwick et al. (2019) recently developed an empirical method to represent sagebrush phenology suitable for drylands of the western US. While this model improved the seasonality of GPP (i.e. GPP activity) in LPJ-GUESS DGVM, it reduced the capability of the model to capture the peak and annual GPP (i.e. GPP capacity). This contrasting performance points to a fundamental concept that modifying phenology or other processes in a DGVM may improve one aspect of the model (e.g. GPP activity) at the expense of others (e.g. GPP capacity). Thus, changing the model structure should be followed by re-evaluating model parameters and other processes (Renwick et al., 2019). One of the shortcomings of the proposed phenology scheme for sagebrush is that it still needs empirical thresholds (e.g., percent of persistent leaves), which might be significantly different among different sites and dependent upon sagebrush species.

Our results show that, at the low productivity site (WBS), the general decadal trend in simulated GPP is coincident with the general trend of precipitation. This is expected in drylands where water is the main limiting factor. This finding is also consistent with an extensive ground-based analysis of this site in Flerchinger et al. (2019) and similar sites (Yan et al., 2019). However, EDv2.2 shows oversensitivity to precipitation at the WBS site, at which small changes in precipitation often leads to sharp changes in the GPP trend. Flerchinger et al. (2019) found that the WBS site is constantly under water stress. A key ecosystem process that mitigates such stress is changing plant community composition in response to interannual variation in precipitation (La Pierre and Smith, 2015; Wilcox et al., 2015). Since representation of such a diverse vegetation community is limited in the EDv2.2 model (i.e. lack of different drylands PFTs), the model is not able to capture such a mitigation strategy in response to precipitation changes. Thus, a solution to the generally exaggerated greening and senescing trends in response to precipitation is to introduce more PFTs to EDv2.2 to better represent the dynamics of vegetation in drylands.

5. Conclusion

In summary, our main conclusion is that at lower elevations, precipitation drives the general trend of GPP which is captured by both MODIS and EDv2.2; however, the model generally exaggerates this trend in comparison to MODIS. Introducing additional PFTs, making structural modification to the model (e.g. phenology scheme), and incorporating land surface processes should increase model applicability at higher elevations. Adding more dryland PFTs will not only contribute to GPP capacity (e.g. forbs in more productive sites) but can also improve estimates of the long-term trends of GPP activity by modifying the landscape composition. The results of this study can contribute to other model benchmarking activities such as the International Land Model Benchmarking (ILAMB) project (Collier et al., 2018). Future studies should focus on combining the capabilities of EDv2.2, remote sensing, and EC flux towers through a data assimilation framework. New satellite products such as solar induced fluorescence (SIF) have great potential to be integrated with DGVMs. Integration of all these sources is necessary for upscaling GPP to the global level (e.g. FLUXCOM project; Jung et al., 2019). The results of this study provide additional guidance for challenges associated with upscaling carbon fluxes in drylands. Considering the heterogeneity of drylands, increasing the number of EC tower sites for calibration and validation will also improve our understanding of GPP capacity and activity.

Funding

This research was funded by NASA Terrestrial Ecology NNX14AD81G, Department of the Interior Northwest Climate Adaptation Science Center graduate fellowship, US Forest Service Western Wildlands Environmental Threat Assessment Center (WWETAC) to Boise State University through Joint Venture Agreement (17-JV-11221633-130), and the Joint Fire Science Program Project ID: 15-1-03-23.

Declaration of Competing Interest

The authors declare that they have no known competing financial interests or personal relationships that could have appeared to influence the work reported in this paper.

Acknowledgments

Field access and support were provided by USDA ARS Northwest Watershed Research Center, NSF EAR 1331872, and NSF EAR 1665519. We would like to acknowledge the high-performance computing support of the R2 compute cluster (DOI: 10.18122/B2S41H) provided by Boise State University's Research Computing Department. Any use of trade, firm, or product names is for descriptive purposes only and does not imply endorsement by the U.S. Government.

Supplementary materials

Supplementary material associated with this article can be found, in the online version, at doi:10.1016/j.agrformet.2020.108270.

References

Ahlström, A., Raupach, M.R., Schurgers, G., Smith, B., Arneth, A., Jung, M., Reichstein, M., Canadell, J.G., Friedlingstein, P., Jain, A.K., Kato, E., Poulter, B., Sitch, S., Stocker, B.D., Viovy, N., Wang, Y.P., Wiltshire, A., Zaehle, S., Zeng, N., 2015. The dominant role of semi-arid ecosystems in the trend and variability of the land CO₂ sink. Science (80-.) 348, 895–899.

Antonarakis, A.S., Munger, J.W., Moorcroft, P.R., 2014. Imaging spectroscopy- and lidar-derived estimates of canopy composition and structure to improve predictions of forest carbon fluxes and ecosystem dynamics. Geophys. Res. Lett. 41, 2535–2542. https://doi.org/10.1002/2013GL058373.

Barnard, D.M., Bauerle, W.L., 2013. The implications of minimum stomatal conductance on modeling water flux in forest canopies. J. Geophys. Res. Biogeosci. 118, 1322–1333. https://doi.org/10.1002/jgrg.20112.

Bonan, G.B., Williams, M., Fisher, R.A., Oleson, K.W., 2014. Modeling stomatal conductance in the earth system: linking leaf water-use efficiency and water transport along the soil-plant-atmosphere continuum. Geosci. Model Dev. 7, 2193–2222. https://doi.org/10.5194/gmd-7-2193-2014.

Botta, A., Viovy, N., Ciais, P., Friedlingstein, P., Monfray, P., 2000. A global prognostic scheme of leaf onset using satellite data. Glob. Chang. Biol. 6, 709–725. https://doi.org/10.1046/j.1365-2486.2000.00362.x.

Brabec, M.A., 2014. Big sagebrush (Artemisia tridentata) in a shifting climate context: assessment of seedling responses to climate.

Campolongo, F., Saltelli, A., 1997. Sensitivity analysis of an environmental model: an application of different analysis methods. Reliab. Eng. Syst. Saf. 57, 49–69. https://doi.org/10.1016/S0951-8320(97)00021-5.

Cariboni, J., Gatelli, D., Liska, R., Saltelli, A., 2007. The role of sensitivity analysis in ecological modelling. Ecol. Modell. 203, 167–182. https://doi.org/10.1016/j.ecolmodel.2005.10.045.

Chen, J., Rao, Y., Shen, M., Wang, C., Zhou, Y., Ma, L., Tang, Y., Yang, X., 2016. A simple method for detecting phenological change from time series of vegetation index. IEEE Trans. Geosci. Remote Sens. 54, 3436–3449. https://doi.org/10.1109/TGRS.2016.2518167.

Collier, N., Hoffman, F.M., Lawrence, D.M., Keppel-Aleks, G., Koven, C.D., Riley, W.J., Mu, M., Randerson, J.T., 2018. The international land model benchmarking (ILAMB) system: design, theory, and implementation. J. Adv. Model. Earth Syst. 10, 2731–2754. https://doi.org/10.1029/2018MS001354.

Comstock, J.P., Ehleringer, J.R., 1992. Plant adaptation in the great basin and colorado plateau. Gt. Basin Nat. 52.

Concilio, A.L., Loik, M.E., Belnap, J., 2013. Global change effects on Bromus tectorum L. (Poaceae) at its high-elevation range margin. Glob. Chang. Biol. 19, 161–172. https://doi.org/10.1111/gcb.12032.

Davidson, E., Lefebvre, P.A., Brando, P.M., Ray, D.M., Trumbore, S.E., Solorzano, L.A., Ferreira, J.N., Bustamante, M.M.D., Nepstad, D.C., 2011. Carbon Inputs and Water Uptake in Deep Soils of an Eastern Amazon Forest. For. Sci. 57, 51–58.

De Kauwe, M.G., Zhou, S.-X., Medlyn, B.E., Pitman, A.J., Wang, Y.-P., Duursma, R.A., Prentice, I.C., 2015. Do land surface models need to include differential plant species responses to drought? Examining model predictions across a mesic-xeric gradient in Europe. Biogeosciences 12, 7503–7518. https://doi.org/10.5194/bg-12-7503-2015.

Dietze, M.C., Serbin, S.P., Davidson, C., Desai, A.R., Feng, X., Kelly, R., Kooper, R., LeBauer, D., Mantooth, J., McHenry, K., Wang, D., 2014. A quantitative assessment of a terrestrial biosphere model's data needs across North American biomes. J. Geophys. Res. Biogeosci. 119, 286–300. https://doi.org/10.1002/2013JG002392.

Doherty, J., 2005. Model independent parameter estimation. fifth edition of user manual. Brisbane,Australia.

Duursma, R.A., Blackman, C.J., Lopéz, R., Martin-StPaul, N.K., Cochard, H., Medlyn, B.E., 2019. On the minimum leaf conductance: its role in models of plant water use, and ecological and environmental controls. New Phytol. 221, 693–705. https://doi.org/10.1111/nph.15395.

Evans, R.D., Black, R.A., 1993. Growth, photosynthesis, and resource investment for vegetative and reproductive modules of artemisia tridentata. Ecology 74, 1516–1528. https://doi.org/10.2307/1940079.

Fang, Q., Ma, L., Harmel, D.R., Yu, Q., Sima, W.M., Bartling, N.S.P., Malone, W.R., Nolan, T.B., Doherty, J., 2019. Uncertainty of CERES-maize calibration under different irrigation strategies using PEST optimization algorithm. Agron. https://doi.org/10.3390/agronomy9050241.

Farquhar, G.D., von Caemmerer, S., Berry, J.A., 1980. A biochemical model of photosynthetic CO2 assimilation in leaves of C3 species. Planta 149, 78–90. https://doi.org/10.1007/BF00386231.

Fer, I., Kelly, R., Moorcroft, P.R., Richardson, A.D., Cowdery, E.M., Dietze, M.C., 2018. Linking big models to big data: efficient ecosystem model calibration through Bayesian model emulation. Biogeosciences 15, 5801–5830. https://doi.org/10.5194/bg-15-5801-2018.

Fisher, R.A., Koven, C.D., Anderegg, W.R.L., Christoffersen, B.O., Dietze, M.C., Farrior, C. E., Holm, J.A., Hurtt, G.C., Knox, R.G., Lawrence, P.J., Lichstein, J.W., Longo, M., Matheny, A.M., Medvigy, D., Muller-Landau, H.C., Powell, T.L., Serbin, S.P., Sato, H., Shuman, J.K., Smith, B., Trugman, A.T., Viskari, T., Verbeeck, H., Weng, E., Xu, C., Xu, X., Zhang, T., Moorcroft, P.R., 2018. Vegetation demographics in earth system models: a review of progress and priorities. Glob. Chang. Biol. https://doi.org/10.1111/gcb.13910.

Flerchinger, G.N., Fellows, A.W., Seyfried, M.S., Clark, P.E., Lohse, K.A., 2019. Water and carbon fluxes along an elevational gradient in a sagebrush ecosystem. Ecosystems. https://doi.org/10.1007/s10021-019-00400-x.

Flerchinger, G.N., Marks, D., Reba, M.L., Yu, Q., Seyfried, M.S., 2010. Surface fluxes and water balance of spatially varying vegetation within a small mountainous headwater catchment. Hydrol. Earth Syst. Sci. 14, 965–978. https://doi.org/10.5194/hess-14-965-2010.

Flores, A., Masarik, M., Watson, K., 2016. A 30-year, multi-domain high-resolution climate simulation dataset for the interior pacific Northwest and Southern Idaho.

Forkel, M., Migliavacca, M., Thonicke, K., Reichstein, M., Schaphoff, S., Weber, U., Carvalhais, N., 2015. Codominant water control on global interannual variability and trends in land surface phenology and greenness. Glob. Chang. Biol. 21, 3414–3435. https://doi.org/10.1111/gcb.12950.

GILL, R.A., JACKSON, R.B., 2000. Global patterns of root turnover for terrestrial ecosystems. New Phytol. 147, 13–31. https://doi.org/10.1046/j.1469-8137.2000.00681.x.

Glenn, N.F., Spaete, L.P., Shrestha, R., Li, A., Ilangakoon, N., MitchelL, J., L, U.S., Qi, Y., Dashti, H., Finan, K., 2017. Shrubland species cover, biometric, carbon and nitrogen data, Southern Idaho, 2014. 10.3334/ornldaac/1503.

Hansen, N., Müller, S.D., Koumoutsakos, P., 2003. Reducing the time complexity of the derandomized evolution strategy with covariance matrix adaptation (CMA-ES). Evol. Comput. 11, 1–18. https://doi.org/10.1162/106365603321828970.

Holben, B.N., 1986. Characteristics of maximum-value composite images from temporal AVHRR data. Int. J. Remote Sens. 7, 1417–1434. https://doi.org/10.1080/01431168608948945.

Hsieh, N.-H., Reisfeld, B., Bois, F.Y., Chiu, W.A., 2018. Applying a global sensitivity analysis workflow to improve the computational efficiencies in physiologically-based pharmacokinetic modeling. Front. Pharmacol. 9, 588. https://doi.org/10.3389/fphar.2018.00588.

Jakeman, A.J., Letcher, R.A., Norton, J.P., 2006. Ten iterative steps in development and evaluation of environmental models. Environ. Model. Softw. 21, 602–614. https://doi.org/10.1016/j.envsoft.2006.01.004.

Janse, J.H., Scheffer, M., Lijklema, L., Van Liere, L., Sloot, J.S., Mooij, W.M., 2010. Estimating the critical phosphorus loading of shallow lakes with the ecosystem model PCLake: sensitivity, calibration and uncertainty. Ecol. Modell. 221, 654–665. https://doi.org/10.1016/j.ecolmodel.2009.07.023.

Jung, M., Schwalm, C., Migliavacca, M., Walther, S., Camps-Valls, G., Koirala, S., Anthoni, P., Besnard, S., Bodesheim, P., Carvalhais, N., Chevallier, F., Gans, F., Groll, D.S., Haverd, V., Ichii, K., Jain, A.K., Liu, J., Lombardozzi, D., Nabel, J.E.M.S., Nelson, J.A., Pallandt, M., Papale, D., Peters, W., Pongratz, J., Rödenbeck, C., Sitch, S., Tramontana, G., Weber, U., Reichstein, M., Koehler, P., O'Sullivan, M., Walker, A., 2019. Scaling carbon fluxes from eddy covariance sites to globe: Synthesis and evaluation of the FLUXCOM approach. Biogeosci. Discuss. 2019, 1–40. https://doi.org/10.5194/bg-2019-368.

Keenan, T.F., Davidson, E.A., Munger, J.W., Richardson, A.D., 2013. Rate my data: quantifying the value of ecological data for the development of models of the terrestrial carbon cycle. Ecol. Appl. 23, 273–286. https://doi.org/10.1890/12-0747.1.

Kim, Y., Knox, R.G., Longo, M., Medvigy, D., Hutyra, L.R., Pyle, E.H., Wofsy, S.C., Bras, R.L., Moorcroft, P.R., 2012. Seasonal carbon dynamics and water fluxes in an Amazon rainforest. Glob. Chang. Biol. 18, 1322–1334. https://doi.org/10.1111/j.1365-2486.2011.02629.x.

Kuppel, S., Peylin, P., Chevallier, F., Bacour, C., Maignan, F., Richardson, A.D., 2012. Constraining a global ecosystem model with multi-site eddy-covariance data. Biogeosciences 9, 3757–3776. https://doi.org/10.5194/bg-9-3757-2012.

La Pierre, K.J., Smith, M.D., 2015. Functional trait expression of grassland species shift with short- and long-term nutrient additions. Plant Ecol. 216, 307–318. https://doi.org/10.1007/s11258-014-0438-4.

Lambrecht, S.C., Shattuck, A.K., Loik, M.E., 2007. Combined drought and episodic freezing effects on seedlings of low- and high-elevation subspecies of sagebrush (Artemisia tridentata). Physiol. Plant. 130, 207–217. https://doi.org/10.1111/j.1399-3054.2007.00904.x.

Leuning, R., 1995. A critical appraisal of a combined stomatal-photosynthesis model for C3 plants. Plant. Cell Environ. 18, 339–355. https://doi.org/10.1111/j.1365-3040.1995.tb00370.x.

Levine, N.M., Zhang, K., Longo, M., Baccini, A., Phillips, O.L., Lewis, S.L., Alvarez-Dávila, E., Segalin de Andrade, A.C., Brienen, R.J.W., Erwin, T.L., Feldpausch, T.R., Monteagudo Mendoza, A.L., Nuñez Vargas, P., Prieto, A., Silva-Espejo, J.E., Malhi, Y., Moorcroft, P.R., 2016. Ecosystem heterogeneity determines the ecological resilience of the Amazon to climate change. Proc. Natl. Acad. Sci. 113, 793–797. https://doi.org/10.1073/pnas.1511344112.

Li, L., van der Tol, C., Chen, X., Jing, C., Su, B., Luo, G., Tian, X., 2013. Representing the root water uptake process in the Common Land Model for better simulating the energy and water vapour fluxes in a Central Asian desert ecosystem. J. Hydrol. 502, 145–155. https://doi.org/10.1016/j.jhydrol.2013.08.026.

Li, L., Wang, Y.-P., Yu, Q., Pak, B., Eamus, D., Yan, J., van Gorsel, E., Baker, I.T., 2012. Improving the responses of the Australian community land surface model (CABLE) to seasonal drought. J. Geophys. Res. Biogeosci. 117 https://doi.org/10.1029/2012JG002038.

Li, Y., Li, L., Dong, J., Bai, J., Yuan, X., Song, S., Zhao, H., Chen, X., Li, Y., 2020. Process refinement contributed more than parameter optimization to improve the CoLM's performance in simulating the carbon and water fluxes in a grassland. Agric. For. Meteorol. 291, 108067 https://doi.org/10.1016/j.agrformet.2020.108067.

Lokupitiya, E., Denning, A.S., Schaefer, K., Ricciuto, D., Anderson, R., Arain, M.A., Baker, I., Barr, A.G., Chen, G., Chen, J.M., Ciais, P., Cook, D.R., Dietze, M., El Maayar, M., Fischer, M., Grant, R., Hollinger, D., Izaurralde, C., Jain, A., Kucharik, C., Li, Z., Liu, S., Li, L., Matamala, R., Peylin, P., Price, D., Running, S.W., Sahoo, A., Sprintsin, M., Suyker, A.E., Tian, H., Tonitto, C., Torn, M., Verbeeck, H., Verma, S.B., Xue, Y., 2016. Carbon and energy fluxes in cropland ecosystems: a model-data comparison. Biogeochemistry 129, 53–76. https://doi.org/10.1007/s10533-016-0219-3.

Longo, M., Knox, R.G., Levine, N.M., Swann, A.L.S., Medvigy, D.M., Dietze, M.C., Kim, Y., Zhang, K., Bonal, D., Burban, B., Camargo, P.B., Hayek, M.N., Saleska, S.R., da Silva, R., Bras, R.L., Wofsy, S.C., Moorcroft, P.R., 2019a. The biophysics, ecology, and biogeochemistry of functionally diverse, vertically- and horizontally-heterogeneous ecosystems: the ecosystem demography model, version 2.2 - Part 2: model evaluation. Geosci. Model Dev. Discuss. 2019, 1–34. https://doi.org/10.5194/gmd-2019-71.

Longo, M., Knox, R.G., Medvigy, D.M., Levine, N.M., Dietze, M.C., Kim, Y., Swann, A.L.S., Zhang, K., Rollinson, C.R., Bras, R.L., Wofsy, S.C., Moorcroft, P.R., 2019b. The biophysics, ecology, and biogeochemistry of functionally diverse, vertically- and horizontally-heterogeneous ecosystems: the ecosystem demography model, version 2.2 — Part 1: model description. Geosci. Model Dev. Discuss. 2019, 1–53. https://doi.org/10.5194/gmd-2019-45.

MacBean, N., Scott, R.L., Biederman, J.A., Ottlé, C., Vuichard, N., Ducharne, A., Kolb, T., Dore, S., Litvak, M., Moore, D.J.P., 2019. Multi-variable, multi-configuration testing of ORCHIDEE land surface model water flux and storage estimates across semi-arid sites in the southwestern US. Hydrol. Earth Syst. Sci. Discuss. 2019, 1–44. https://doi.org/10.5194/hess-2019-598.

Medvigy, D., Clark, K.L., Skowronski, N.S., Schäfer, K.V.R., 2012. Simulated impacts of insect defoliation on forest carbon dynamics. Environ. Res. Lett. 7, 45703. https://doi.org/10.1088/1748-9326/7/4/045703.

Medvigy, D., Jeong, S.-J., Clark, K.L., Skowronski, N.S., Schäfer, K.V.R., 2013. Effects of seasonal variation of photosynthetic capacity on the carbon fluxes of a temperate deciduous forest. J. Geophys. Res. Biogeosci. 118, 1703–1714. https://doi.org/10.1002/2013JG002421.

Medvigy, D., Wofsy, S.C., Munger, J.W., Hollinger, D.Y., Moorcroft, P.R., 2009a. Mechanistic scaling of ecosystem function and dynamics in space and time: ecosystem demography model version 2. J. Geophys. Res. 114, G01002. https://doi.org/10.1029/2008JG000812.

Medvigy, D., Wofsy, S.C., Munger, J.W., Hollinger, D.Y., Moorcroft, P.R., 2009b. Mechanistic scaling of ecosystem function and dynamics in space and time: ecosystem demography model version 2. J. Geophys. Res. 114, G01002. https://doi.org/10.1029/2008JG000812.

Metcalfe, D.B., 2014. A sink down under. Nature 509, 566.

Migliavacca, M., Sonnentag, O., Keenan, T.F., Cescatti, A., O'Keefe, J., Richardson, A.D., 2012. On the uncertainty of phenological responses to climate change, and implications for a terrestrial biosphere model. Biogeosciences 9, 2063–2083. https://doi.org/10.5194/bg-9-2063-2012.

Moorcroft, P.R., Hurtt, G.C., Pacala, S.W., 2001. A method for scaling vegetation dynamics: the ecosystem demography model (ED). Ecol. Monogr. 71, 557–586. https://doi.org/10.1890/0012-9615(2001)071[0557:AMFSVD]2.0.CO;2.

Oleson, K., Lawrence, D.M., Bonan, G.B., Drewniak, B., Huang, M., Koven, C.D., Levis, S., Li, F., Riley, W.J., Subin, Z.M., Swenson, S.C., Thornton, P.E., Bozbiyik, A., Fisher, R., Heald, C.L., Kluzek, E., Lamarque, J.-F., Lawrence, P.J., Leung, L.R., Lipscomb, W., Muszala, S., Ricciuto, D.M., Sacks, W., Sun, Y., Tang, J., Yang, Z.-L., 2013. Technical description of version 4.5 of the community land model (CLM). NCAR Tech. Note NCAR/TN-503+STR 420.

Olsoy, P.J., Mitchell, J.J., Levia, D.F., Clark, P.E., Glenn, N.F., 2016. Estimation of big sagebrush leaf area index with terrestrial laser scanning. Ecol. Indic. 61, 815–821. https://doi.org/10.1016/j.ecolind.2015.10.034.

Pandit, K., Dashti, H., Glenn, N.F., Flores, A.N., Maguire, K.C., Shinneman, D.J., Flerchinger, G.N., Fellows, A.W., 2019a. Developing and optimizing shrub parameters representing sagebrush (Artemisia spp.) ecosystems in the northern great basin using the ecosystem demography (EDv2.2) model. Geosci. Model Dev. 12, 4585–4601. https://doi.org/10.5194/gmd-12-4585-2019.

Pandit, K., Dashti, H., Glenn, N.F., Flores, A.N., Maguire, K.C., Shinneman, D.J., Flerchinger, G.N., Fellows, A.W., 2019b. Optimizing shrub (Sagebrush) parameters to estimate gross primary production of sagebrush-steppe ecosystem using Ecosystem Demography (ED2) model. Geosci. Model Dev. Accepted f.

Pappas, C., Fatichi, S., Leuzinger, S., Wolf, A., Burlando, P., 2013. Sensitivity analysis of a process-based ecosystem model: pinpointing parameterization and structural issues. J. Geophys. Res. Biogeosci. 118, 505–528. https://doi.org/10.1002/jgrg.20035.

Polley, H.W., Briske, D.D., Morgan, J.A., Wolter, K., Bailey, D.W., Brown, J.R., 2013. Climate change and North American rangelands: trends, projections, and implications. Rangel. Ecol. Manag. 66, 493–511. https://doi.org/10.2111/REM-D-12-00068.1.

Post, H., Vrugt, J.A., Fox, A., Vereecken, H., Hendricks Franssen, H.-J., 2017. Estimation of community land model parameters for an improved assessment of net carbon fluxes at European sites. J. Geophys. Res. Biogeosci. 122, 661–689. https://doi.org/10.1002/2015JG003297.

Poulter, B., Frank, D., Ciais, P., Myneni, R.B., Andela, N., Bi, J., Broquet, G., Canadell, J. G., Chevallier, F., Liu, Y.Y., Running, S.W., Sitch, S., Van Der Werf, G.R., 2014. Contribution of semi-arid ecosystems to interannual variability of the global carbon cycle. Nature 509. https://doi.org/10.1038/nature13376.

Renwick, K.M., Fellows, A., Flerchinger, G.N., Lohse, K.A., Clark, P.E., Smith, W.K., Emmett, K., Poulter, B., 2019. Modeling phenological controls on carbon dynamics in dryland sagebrush ecosystems. Agric. For. Meteorol. 274, 85–94. https://doi.org/10.1016/j.agrformet.2019.04.003.

Richardson, A.D., Keenan, T.F., Migliavacca, M., Ryu, Y., Sonnentag, O., Toomey, M., 2013. Climate change, phenology, and phenological control of vegetation feedbacks to the climate system. Agric. For. Meteorol. 169, 156–173. https://doi.org/10.1016/j.agrformet.2012.09.012.

Running, S., Nemani, R., Heinsch, F.A.N.N., Zhao, M., REEVES, M., Hashimoto, H., 2004. A continuous satellite-derived measure of global terrestrial primary production. Bioscience 54, 547–560. https://doi.org/10.1641/0006-3568(2004)054[0547:ACSMOG]2.0.CO;2.

Ryu, Y., Berry, J.A., Baldocchi, D.D., 2019. What is global photosynthesis? History, uncertainties and opportunities. Remote Sens. Environ. 223, 95–114. https://doi.org/10.1016/j.rse.2019.01.016.

Saltelli, A., Tarantola, S., Campolongo, F., 2000. Sensitivity analysis as an ingredient of modeling. Stat. Sci. 15, 377–395.

Santaren, D., Peylin, P., Viovy, N., Ciais, P., 2007. Optimizing a process-based ecosystem model with eddy-covariance flux measurements: a pine forest in southern France. Glob. Biogeochem. Cycles 21. https://doi.org/10.1029/2006GB002834.

Scott, R.L., Biederman, J.A., Hamerlynck, E.P., Barron-Gafford, G.A., 2015. The carbon balance pivot point of southwestern U.S. semiarid ecosystems: insights from the 21st century drought. J. Geophys. Res. Biogeosci. 120, 2612–2624. https://doi.org/10.1002/2015JG003181.

Shiklomanov, A.N., Bond-Lamberty, B., Atkins, J.W., Gough, C.M., 2020. Structure and parameter uncertainty in centennial projections of forest community structure and carbon cycling. Glob. Chang. Biol. n/a https://doi.org/10.1111/gcb.15164.

Smith, W.K., Biederman, J.A., Scott, R.L., Moore, D.J.P., He, M., Kimball, J.S., Yan, D., Hudson, A., Barnes, M.L., MacBean, N., Fox, A.M., Litvak, M.E., 2018. Chlorophyll fluorescence better captures seasonal and interannual gross primary productivity dynamics across dryland ecosystems of Southwestern North America. Geophys. Res. Lett. 45, 748–757. https://doi.org/10.1002/2017GL075922.

Stocker, B.D., Zscheischler, J., Keenan, T.F., Prentice, I.C., Seneviratne, S.I., Peñuelas, J., 2019. Drought impacts on terrestrial primary production underestimated by satellite monitoring. Nat. Geosci. 12, 264–270. https://doi.org/10.1038/s41561-019-0318-6.

Storn, R., Price, K., 1997. Differential evolution - a simple and efficient heuristic for global optimization over continuous spaces. J. Glob. Optim. 11, 341–359. https://doi.org/10.1023/A:1008202821328.

Swenson, S.C., Lawrence, D.M., 2014. Assessing a dry surface layer-based soil resistance parameterization for the community land model using GRACE and FLUXNET-MTE data. J. Geophys. Res. Atmos. 119 (10), 210–299. https://doi.org/10.1002/2014JD022314, 312.

Tian, Y., Hassmiller Lich, K., Osgood, N.D., Eom, K., Matchar, D.B., 2016. Linked sensitivity analysis, calibration, and uncertainty analysis using a system dynamics model for stroke comparative effectiveness research. Med. Decis. Mak. 36, 1043–1057. https://doi.org/10.1177/0272989X16643940.

Trugman, A.T., Fenton, N.J., Bergeron, Y., Xu, X., Welp, L.R., Medvigy, D., 2016. Climate, soil organic layer, and nitrogen jointly drive forest development after fire in the North American boreal zone. J. Adv. Model. Earth Syst. 8, 1180–1209. https://doi.org/10.1002/2015MS000576.

Verma, M., Friedl, M.A., Richardson, A.D., Kiely, G., Cescatti, A., Law, B.E., Wohlfahrt, G., Gielen, B., Roupsard, O., Moors, E.J., Toscano, P., Vaccari, F.P., Gianelle, D., Bohrer, G., Varlagin, A., Buchmann, N., van Gorsel, E., Montagnani, L., Propastin, P., 2014. Remote sensing of annual terrestrial gross primary productivity from MODIS: an assessment using the FLUXNET La Thuile data set. Biogeosciences 11, 2185–2200. https://doi.org/10.5194/bg-11-2185-2014.

Wang, D., LeBauer, D., Dietze, M., 2013. Predicting yields of short-rotation hybrid poplar (Populus spp.) for the United States through model-data synthesis. Ecol. Appl. 23, 944–958. https://doi.org/10.1890/12-0854.1.

Wang, Y.-P., Leuning, R., Cleugh, H.A., Coppin, P.A., 2001. Parameter estimation in surface exchange models using nonlinear inversion: how many parameters can we estimate and which measurements are most useful? Glob. Chang. Biol. 7, 495–510. https://doi.org/10.1046/j.1365-2486.2001.00434.x.

White, J., Welter, D., Doherty, J., 2019. PEST++: version 4.2.1.

Wilcox, K.R., Blair, J.M., Smith, M.D., Knapp, A.K., 2015. Does ecosystem sensitivity to precipitation at the site-level conform to regional-scale predictions? Ecology 0. https://doi.org/10.1890/15-1437.

Williams, R.J., Myers, B.A., Muller, W.J., Duff, G.A., Eamus, D., 1997. Leaf phenology of woody species in a North Australian tropical savanna. Ecology 78, 2542–2558. https://doi.org/10.1890/0012-9658(1997)078[2542:LPOWSI]2.0.CO;2.

Wu, G.-L., Huang, Z., Liu, Y.-F., Cui, Z., Liu, Y., Cheng, X., Tian, F.-P., López-Vicente, M., Shi, Z.-H., 2019. Soil water response of plant functional groups along an artificial legume grassland succession under semi-arid conditions.

Wu, G.-L., López-Vicente, M., Huang, Z., Cui, Z., Liu, Y., 2020. Preferential water flow through decayed root channels enhances soil water infiltration: evaluation in distinct vegetation types under semi-arid conditions. Hydrol. Earth Syst. Sci. Discuss. 2020, 1–22. https://doi.org/10.5194/hess-2020-266.

Xu, X., Medvigy, D., Powers, J.S., Becknell, J.M., Guan, K., 2016. Diversity in plant hydraulic traits explains seasonal and inter-annual variations of vegetation dynamics in seasonally dry tropical forests. New Phytol. 212, 80–95. https://doi.org/10.1111/nph.14009.

Yan, D., Scott, R.L., Moore, D.J.P., Biederman, J.A., Smith, W.K., 2019. Understanding the relationship between vegetation greenness and productivity across dryland ecosystems through the integration of PhenoCam, satellite, and eddy covariance data. Remote Sens. Environ. 223, 50–62. https://doi.org/10.1016/j.rse.2018.12.029.

Yao, J., Liu, H., Huang, J., Gao, Z., Wang, G., Li, D., Yu, H., Chen, X., 2020. Accelerated dryland expansion regulates future variability in dryland gross primary production. Nat. Commun. 11, 1665. https://doi.org/10.1038/s41467-020-15515-2.

Zhang, K., de Almeida Castanho, A.D., Galbraith, D.R., Moghim, S., Levine, N.M., Bras, R. L., Coe, M.T., Costa, M.H., Malhi, Y., Longo, M., Knox, R.G., McKnight, S., Wang, J., Moorcroft, P.R., 2015. The fate of Amazonian ecosystems over the coming century arising from changes in climate, atmospheric CO2, and land use. Glob. Chang. Biol. https://doi.org/10.1111/gcb.12903.

Zhao, K., Wulder, M.A., Hu, T., Bright, R., Wu, Q., Qin, H., Li, Y., Toman, E., Mallick, B., Zhang, X., Brown, M., 2019. Detecting change-point, trend, and seasonality in satellite time series data to track abrupt changes and nonlinear dynamics: a Bayesian ensemble algorithm. Remote Sens. Environ. 232, 111181 https://doi.org/10.1016/j.rse.2019.04.034.